Permeability and damage of partially saturated concrete exposed to elevated temperature

Hognon Sogbossi, Jérôme Verdier, Stéphane Multon

To cite this version:

Hognon Sogbossi, Jérôme Verdier, Stéphane Multon. Permeability and damage of partially saturated concrete exposed to elevated temperature. Cement and Concrete Composites, 2020, 109, pp.103563. 10.1016/j.cemconcomp.2020.103563 . hal-02617082

HAL Id: hal-02617082
https://hal.insa-toulouse.fr/hal-02617082

Submitted on 27 Sep 2023

Permeability and damage of partially saturated concrete exposed to elevated temperature

Hognon Sogbossi, Jérôme Verdier, Stéphane Multon*

LMDC, Université de Toulouse, INSA, UPS, 135 Avenue de Rangueil, 31077 Toulouse cedex 04, France

---

Abstract

This work analyses the impact of elevated temperature on the permeability and on the damage of concrete according to its saturation degree. The Young Modulus and gas permeability were measured on samples with different initial saturation degrees that were subjected to thermal loading (80, 150 and 200 °C). These conditions were defined to simulate the hydrothermal loading of nuclear plant concrete in case of accident. To analyse the behaviour of concrete exposed to high temperature, it is necessary to distinguish the effects of water saturation and the impact of damage on permeability. Experimentations shows that concrete with high saturation degree can be permeable to air after thermal loading, while it was not permeable before the loading. Relations are proposed to link the permeability variation to temperature according to the initial saturation degree of the concrete and to evaluate the permeability variation from the induced damage.

Keywords: *Damage; Durability; Permeability; Saturation degree; Temperature; Transport Properties*

---

*Corresponding author: Email: multon@insa-toulouse.fr

1 Introduction

Permeability quantifies the fluid flow through a porous medium under the effect of a pressure gradient. Sealing quality of concrete is an important property for specific structures. Permeability can also be used to evaluate the durability performance of concrete.

Thermal loading due to temperature increase is an important risk for structures. The heating may be caused by fire or by accidental situations in nuclear power plants leading to loss of coolant accidents (LOCA). Thermal loading (increase of temperature expected from 20 °C up to 200 °C in case of LOCA) can lead to important cracking. Sealing is of prime importance for the enclosure vessels of nuclear power plants. After LOCA and resulting thermal loading, the increase of permeability due to induced thermal cracking leads to the decrease of sealing capacity. This consequence has to be evaluated to ensure the security of the equipment. The evaluation of the increase of permeability according to thermal loading is the main objective of this study.

Exposure to high temperature and the resulting drying lead to many evolutions in the micro and macro-structure of concrete. These evolutions have various consequences on mechanical properties [1-5] and permeability [6-12].

Different origins can explain the damage induced by thermal loading: physicochemical origin (decomposition of hydrates [13-16]), micromechanical origin leading to cracking (in the interfacial transition zone due to differential dilation of aggregate and cement paste [17, 18], due to drying shrinkage of paste restrained by aggregate [8], or due to the increase in vapour pressure [19, 20]) and macro mechanical origin leading to structural cracking (temperature and humidity gradient [21]). In modelling, damage during thermal loading is thus evaluated from dehydration and crack development induced by thermally induced microcracking [10, 18, 22].

During drying, the reduction of the water content by evaporation due to heating [5, 23] leads also to an increase of free porosity. It has a strong impact on the connection of natural percolation paths and thus on permeability [24, 25]. The evolution of the concrete permeability after thermal loading may be regarded as a function of the accessible gas porosity due to water removal on the one hand, and as a function of diffuse micro-cracking in the material on the other [15]. The width, connectivity and tortuosity of old and newly created flow channels determine the concrete permeability after the loading.

Water content in concrete is adapted to obtain correct rheology during casting. As a consequence, the saturation degree of concrete is high even when cement hydration is advanced (usual concrete saturation lies between 75 and 90% for hydration degrees upper than 80%). The degree of saturation of concrete stays usually high in the cores of massive structures and in locations submitted to rainfall (over 80% at 50 mm depth [26]). For lower, but current, external environmental conditions (between 50 and 60% of relative humidity), the saturation of most concrete lies also between 50 and 60%. The loss of coolant accidents (LOCA) can occur at any time of the service life of the structures. Before the accident, the saturation degree of concrete skin of the internal enclosure vessel is about 60%. The saturation degree of the core of these massive walls (about 1 meter width) can be expected between 60 and 80% [27, 28]. It is thus important to evaluate the response of the concrete exposed to elevated temperature with high initial saturation degrees.

The impact of temperature, saturation degree and thermal loading on concrete permeability has been widely studied and analysed in the literature [6-12, 29-35]. However, cementitious materials subjected to thermal loading in the previous experimental programs have low saturation degrees [7, 36]. The impact of exposure temperature on the permeability of partially saturated concrete has been little studied while the water saturation of porosity should have a major impact on overpressure due to thermal heating. The experimental program presented in this paper attempts to test the material under conditions close to those found in situ: the concrete is partially saturated with water at the time of the thermal loading. This gap has to be filled to be able to evaluate the containment properties after thermal loading of in situ concrete. The evolutions of the permeability and modulus of elasticity of concrete are presented and analysed. Correlation of the evolution of permeability of concrete exposed to elevated temperatures with the evolution of mechanical properties is also an important result of this study.

2 Materials and methods

2.1 Composition of concrete mix

Concrete used in this work (Table 1) is representative of a wide range of concrete used in French nuclear plants. It is the same mix that the concrete used for the Vercors mockup built by EDF to help the management of long term operation of its fleet of Nuclear Power Plants [37]. Siliceous limestone aggregates were used. Silica contents of aggregates were about 80 and 5% for the sand and the gravels, respectively [38]. Twenty-four hours after casting, the samples were removed from their moulds and cured in lime water at a temperature of 20 ± 2 °C for at least 60 days. This long period in lime water was required to obtain a stabilized material regarding cement hydration [39]. The mean compressive strength of the concrete was 42 MPa.

Table 1. Concrete mix

Constituents	**[kg/m^3]**
Sand 0/4	830
Gravel 4/11 R	445
Gravel 8/16 R	550
Cement CEM I 52.5 NCE CP2 NF	320
Plasticizer	2.4
Water	167

2.2 Conditioning

The aim of this study was to apply thermal loading to concrete with different initial saturation degrees. To control the saturation degree, the samples were exposed to drying. Such drying can generate moisture gradient, which can affect air permeability, particularly if moisture content is high. Samples underwent thus precise conditioning. This conditioning was inspired by the literature [40-42] and was intended to limit the thermo-hydric gradient and resulting skin cracking during conditioning before the tests.

First, the samples were fully saturated under vacuum. Then, the samples were dried in an oven with a gradually increasing drying temperature (40 °C to reach 80%, 60 °C to reach, 60%, 30 and 10%, 105 °C to obtain the smallest degree of saturation assumed to be 0% in this work). The targeted masses were determined from the concrete porosity measured on other samples casted during the same concrete batch, before the conditioning of samples exposed to elevated temperatures. Once the target mass was reached, samples were packed in aluminium and sealed bags. Then, they were put back into the oven for a period of time at least equal to the drying time under watertight sealing in order to partially rehomogenize the water distribution throughout the sample and thus minimize the impact of moisture gradient on air permeability measurements [42].

The dry state (S_0 = 0%) can only be achieved with a conditioning temperature of 105 °C. Such a temperature can lead to significant cracking [43]. It is confirmed in this experimental study. The impact on the results of modulus and permeability are thus discussed in the analysis.

2.3 Methods

2.3.1 Modulus

In this work, the evolution of the concrete mechanical property is evaluated by the modulus of elasticity. It was measured on cylindrical specimens (diameter: 110 mm, height: 220 mm) according to the European standard [44]. The longitudinal deformation of the samples was measured with three gauges (KC 70 – 120- A1-11 having a gauge factor of 2.11 $\pm$ 1%). Gauges were stuck vertically and equidistant from one another on the lateral surface of the samples. The compression test was carried out using a hydraulic cylinder mechanical press with a capacity of 4000 kN. The force was applied in autopilot mode with force control at the speed of 0.5 MPa/s, respecting the CPC8 recommendations [45], which advise testing the specimen at 30% of the breaking load over five loading/unloading cycles. The elastic modulus was calculated on the last increase in load (5th cycle) from the following relation:

$$E = \frac{\sigma_{30} - \sigma_0}{\varepsilon_{30} - \varepsilon_0} \qquad \textit{Eq. 1}$$

where σ_{30} is equal to 30% of the compressive strength; σ_0 is the strain preload of the press, which is equal to 0.5 MPa; ε_{30} is the longitudinal strain corresponding to stress σ_{30} of the 5th cycle; and ε_0 is the longitudinal strain corresponding to stress σ_0 of the 5th cycle.

2.3.2 Permeability

The permeability was measured with a Cembureau permeameter. After the curing period, the samples (diameter =150 mm, h=50 mm) were sawn from the original cylindrical specimens (diameter =150 mm, h = 200 mm) and the first 20 mm of both ends were removed to avoid skin effects. The coefficient of permeability was defined by the Darcy law and the gas apparent permeability of a porous medium was calculated using the Hagen-Poiseuille relationship for laminar flow of a compressible fluid through a porous medium with small capillaries under steady-state conditions [46]:

$$k = \frac{2\,\mu\,L}{S({P_I}^2 - {P_O}^2)} P_a Q_O \qquad \textit{Eq. 2}$$

where k is the apparent permeability obtained for $P_I = 2\ bars$ according to standard [47], $P_a Q_O$ is the outlet gaseous flow, P_I and P_O are inlet and outlet pressures with P_O equal to atmospheric pressure P_a, S is the cross-sectional area of the specimen (m^2), L is the thickness of the specimen in the direction of flow (m), μ is the dynamic viscosity of the fluid ($N.s.m^{-2}$).

2.4 Experimental program

2.4.1 Impact of drying on modulus and permeability

The Young modulus and the permeability of the concrete was first measured for four saturation states: Sw = 100%, 60%, 30%, and 00% without thermal loading. It is necessary to quantify the effect of the drying obtained with moderate and progressive heating on the properties before the application of the thermal loading. The drying was applied to samples (diameter: 110 mm, height: 220 mm for the mechanical characterization and diameter: 150 mm, h: 50 mm for the transfer measurements) after a minimum of 60 days of curing in lime water in order to reach a stabilized material regarding hydration. The drying durations were determined according to temperature of conditioning to obtain the mass for the targeted saturation degrees as explained in the ‘conditioning’ part.

2.4.2 Impact of thermal loading on modulus and permeability

This part of the experimental program concerns the determination of the evolution of the Young modulus and of the permeability after thermal loading. The thermal loading was applied to samples (same sizes than for the study of drying) with four initial degrees of saturation (100, 60, 30, and 00%) after 60 days of curing in lime water. Each sample was wrapped in aluminium and subjected to the thermal loading in an oven preheated to the target temperature T. The samples were directly exposed to the temperature in the oven. The duration of the thermal loading was 14 hours. This heating time was defined on the basis of experience gained on the slabs of the ENDE project [48]. The 14-hour duration allowed the target temperature to be reached and to be maintained for two hours in the specimen cores. The mechanical and permeability tests were performed after the return to ambient temperature. For a given temperature, three samples were tested per initial saturation degree.

The Young modulus was measured after thermal loading for three temperatures: T = 80, 150 and 200 °C.

For the permeability measurements, twelve different samples (diam: 150 mm, h: 50 mm) were tested. The samples were first exposed to the thermal loading at 80 °C, then at 150 °C and finally at 200 °C. Before the exposition at 200 °C, the samples were resaturated to their initial saturation degree as explained just below. Permeability tests were performed between each exposure temperature and the next.

Samples were packed in aluminium foil to limit the loss of water during the exposure. After the thermal loading at 80 °C, no loss of mass was noted for any of the samples. All the water stayed in the concrete during the exposure at 80 °C, and the permeability tests were performed at the initial saturation degree (Sw0). After the permeability measurements, the same samples were exposed to the second thermal loading (150 °C). After the exposure at 150 °C and 200 °C, samples lost all their water content. It was decided to perform permeability tests after the return to ambient temperature for two saturation degrees:

- The first permeability test (K1) was performed directly after the thermal loading. This measurement was thus representative of dry concrete.
- The second permeability test (K2) was performed after resaturation: the permeability measurement was performed with the water content present before the temperature exposure and was representative of concrete exposed to steam and air during an accident [49, 50] and saturated again due to natural humid conditions after the accident.

The samples were exposed to the third thermal loading (200 °C) after the permeability test K2 and thus on samples resaturated to their initial saturation degree.

In order to characterize the mechanisms at high saturation degree, three samples were subjected to the chosen temperature with 100% of saturation in order to simulate the case of the highest impact of water vapour. Permeability tests were then performed with 80% of saturation since there is no percolation path for gas when the material is entirely full of water (100%). At 80% of saturation, concrete permeability can be measured if the damage induced by the thermal loading is sufficient.

3 Experimental results

3.1 Modulus

3.1.1 Evolution with the saturation degree

The evolution of the mechanical properties with the saturation degree has been well studied in the literature [1-5, 51-58]. Most of the previous studies point out an increase in strength [51-55, 58] and a decrease in Young modulus [52-55, 57, 58]. In concrete submitted to drying, two main mechanisms are in competition: the strengthening of material by capillary forces and surface tension, and the damage of concrete due to micro-cracking induced by drying [1, 8, 51-53]. The first mechanism is preponderant in the strength evolution while the second mechanism has an important impact on modulus [53]. The contribution of water compressibility could also participate to greater modulus of the saturated concrete compared to dry material [58]. In some cases, a rare small increase of modulus can be observed for dry concrete [56, 59].

In this study, it was important to characterize the dependence of the Young modulus on the saturation degree in order to separate the impact of the temperature and the effect of the saturation degree in the following analysis. The results are in good agreement with the literature with a decrease of modulus with the saturation degree (Figure 1).

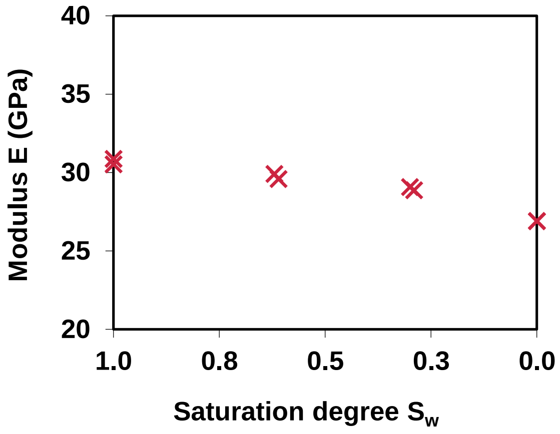

Figure 1.Evolution of modulus E as a function of the saturation degree S_w

3.1.2 Evolution after thermal loading

The mechanical properties were measured on the concrete before and after exposure to three temperatures (80 °C, 150 °C and 200 °C) for four initial saturation states (100%, 60%, 30% and 00%). The evolution of the modulus is represented as a function of temperature in Figure 2. The results of the previous part have been added (T = 60 °C for samples E30, E60, E100 and T = 105 °C for samples E00) for comparison with the three thermal loading. For a given initial degree of saturation (Figure 2), the modulus of elasticity decreases significantly with the increase in temperature, as expected from the literature.

The initial saturation state seems to have little impact on the evolution of the modulus. For high temperature, water vaporization occurs. For such small specimens, vapour moves out of the concrete quickly during drying and the impact of the pressure induced in the concrete is minimal. These tests were representative of concrete skin directly exposed to high temperatures or for elements with small thickness. They may not be representative of what happens in the core of a massive structure [19], although the vapour present in these areas could also migrate through the steel concrete-interfaces [60] in cases of severe thermal loads [61].

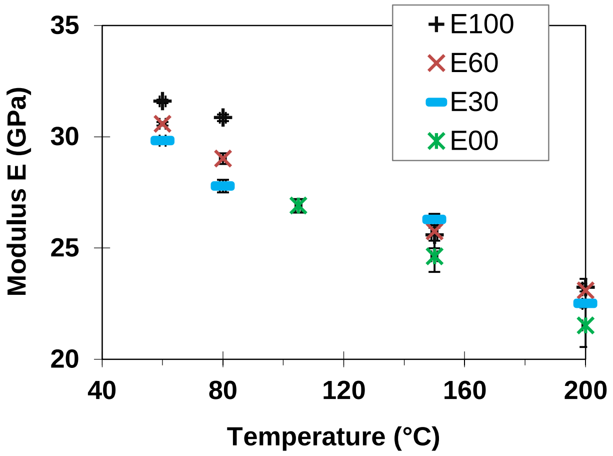

Figure 2. Evolution of the modulus E according to the temperature for four initial saturation degrees

3.2 Permeability

3.2.1 Evolution with the saturation degree

The apparent permeability of all the samples was first tested before the thermal loading, just after the preconditioning at 40 or 60 °C (Figure 3) in order to quantify the variation of permeability with the saturation state. Experimental values are given in Figure 3-a versus the saturation degree. They were used as references in the following analysis of the impact of temperature on permeability. Even if the conditioning protocol uses moderate drying, it induces micro-cracking, which modifies the percolation network. The increase of permeability is thus due to the combination of the water departure and the cracking. The results are in good agreement with previous experimental and numerical works [34, 60, 62, 63].

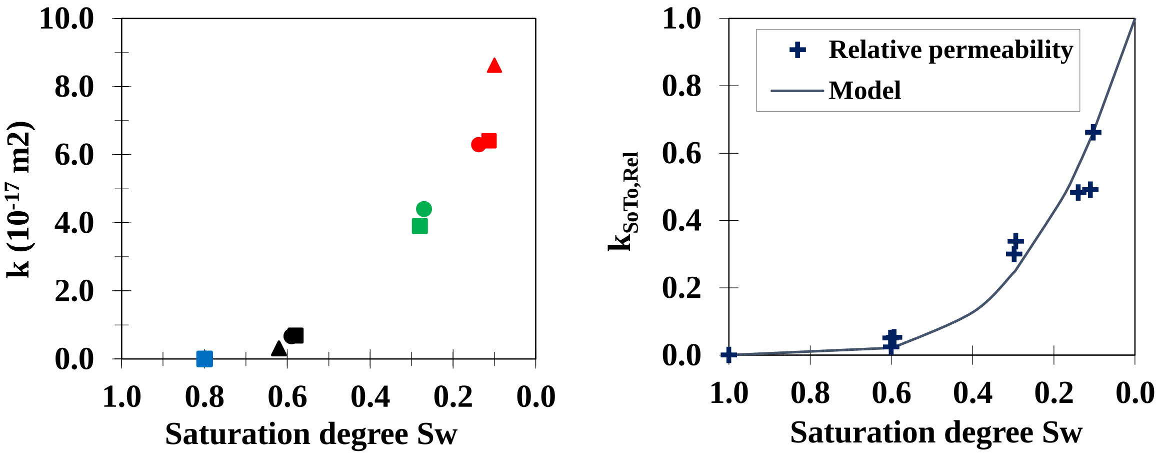

(a) (b)

Figure 3. Evolution of apparent permeability k as a function of the saturation degree (a) and relative permeability (b)

Usual dispersion was observed for most samples, particularly at 10% of saturation. It can be explained by the heterogeneity of the concrete in terms of microstructure and, more particularly, of porosity paths accessible to gas. The heterogeneity increased with drying.

From these experimental results, the relative permeability was defined (Figure 3-b):

$$k_{S_0T_0\_Rel} = \frac{k_{S_0}}{k_0} \qquad \textit{Eq. 3}$$

where $k_{S_0T_0\_Rel}$ is the relative permeability for the saturation degree S_0, k_{S_0} is the apparent permeability for the samples at the saturation degree S_0 and k_0 is the apparent permeability in the dry state.

One of the main difficulties was to obtain the apparent permeability k_0 representative of the concrete studied. The dry state (S_0 = 0%) was obtained with a conditioning temperature of 105 °C. This drying leads to cracking and this state was not representative of the initial state of concrete subjected to the thermal loading in the following experiments (exposed to less than 60 °C before the loading). To obtain relevant and representative analysis, k_0 was evaluated from the permeability measurements obtained for conditioning temperatures lower than or equal to 60 °C. A van Genuchten model [64] was used to deduce the corresponding k_0 (Figure 3-b):

$$k_{S_0T_0} = k_0 \cdot \underbrace{(1 - S_w)^q \left(1 - {S_w}^{1/m}\right)^{2m}}_{k_{S_0T_{0}{}_{Rel}}} \qquad \textit{Eq. 4}$$

where $k_{So,To}$ is the apparent permeability for a given saturation degree S_{w0}. q and m are the van Genuchten parameters, which depend on material characteristics.

For the concrete tested in this study, the apparent permeability k_0 obtained from the van Genuchten model on samples conditioned at less than 60 °C was equal to 13.10^{-17} m^2. q and m were respectively equal to 3.7 and 0.5. These values are in good agreement with usual literature values (q lies between 3.5 and 5 and m is equal to 0.5 [35, 65-67]). Apparent permeability in the dry state (0% of saturation) after drying at 105 °C was also measured at the end of the experimentation. It was equal to more than $18.5.10^{-17}$ m^2 (with a standard deviation of about 6.10^{-17} m^2). The difference between the permeability deduced from the van Genuchten model and the permeability measurement after the conditioning at 105 °C can be explained by the impact of the damage on transfer properties of concrete when the temperature of conditioning becomes too high. For such temperatures, the origin of the damage changes: considerable thermo-chemical damage is then combined with hydric damage. This leads to strong nonlinearity for damage (Figure 1) and for permeability.

3.2.2 Evolution of permeability just after thermal loading

Permeability measured on samples just after the thermal loading (K1) is presented in Figure 4 for the four saturation degrees.

The aim of this part was to quantify the permeability variation measured on dry samples. It was only achieved for 150 and 200 °C (specimens exposed to 80 °C were not dry at the end of the temperature exposure and are thus not analysed in this part). A thermal loading of 200 °C led to a greater increase in permeability than 150 °C (Figure 4). Such results can be explained by the increase in the thermo-chemical damage between 150 and 200 °C.

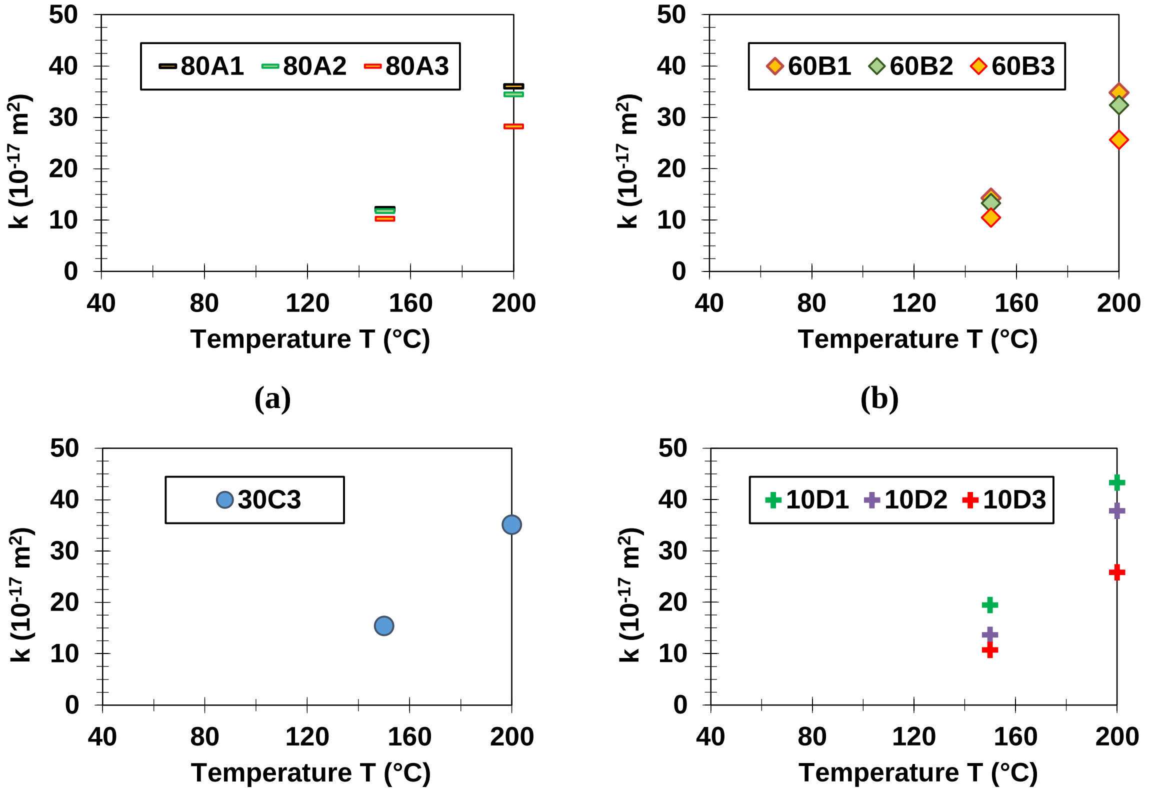

(a) (b) (c) (d)

Figure 4. Apparent permeability just after thermal loading at 150 and 200 °C for four initial saturation degrees

After thermal loading at 150 and 200 °C, the permeability of samples lies in the same range whatever their initial saturation degree (Figure 4). As for mechanical characterization, samples lost free and combined water quickly and the difference of initial saturation degree had little impact. The temperature of loading seems to play the major role in the permeability increase when permeability is measured in the dry state. To distinguish the impact of the saturation degree of concrete during measurement and the effect of damage, permeability measurements were performed after resaturation (protocol K2). This is presented in the following section.

3.2.3 Evolution of permeability after resaturation

The permeability of the samples measured after the resaturation of the concrete with the same quantity of water (protocol K2) is presented in Figure 5.

Apparent permeability is small, and lower than permeability obtained for K1 in Figure 4. This result was to be expected as the saturation degree increased between the two protocols of measurement. Large relative increases have to be noted for high saturation degrees (Figure 5). For saturation degrees of concrete equal to 60 or 80% during measurement (samples 60Bi and 80Ai in Figure 5), permeability was hardly measurable at initial temperature because very little flow could cross the samples. However, after exposure to 150 and 200 °C, flow was clearly detectable while the saturation degree was still high (Figure 5).

Thermal loading below 100 °C seems to have little impact on air permeability. As samples were conditioned at 50°C to reach their target saturation degree the impact of thermal stress on percolation paths between 50°C and the thermal loading at 80°C was not sufficient to lead to a change in permeability. After thermal loading at 150 °C and 200 °C, the permeability increased for all the saturation degree as already observed for dry concrete in [68]. Physicochemical degradation and mechanical damage increased the accessible porosity and modified the concrete microstructure, so an increase of permeability was observed.

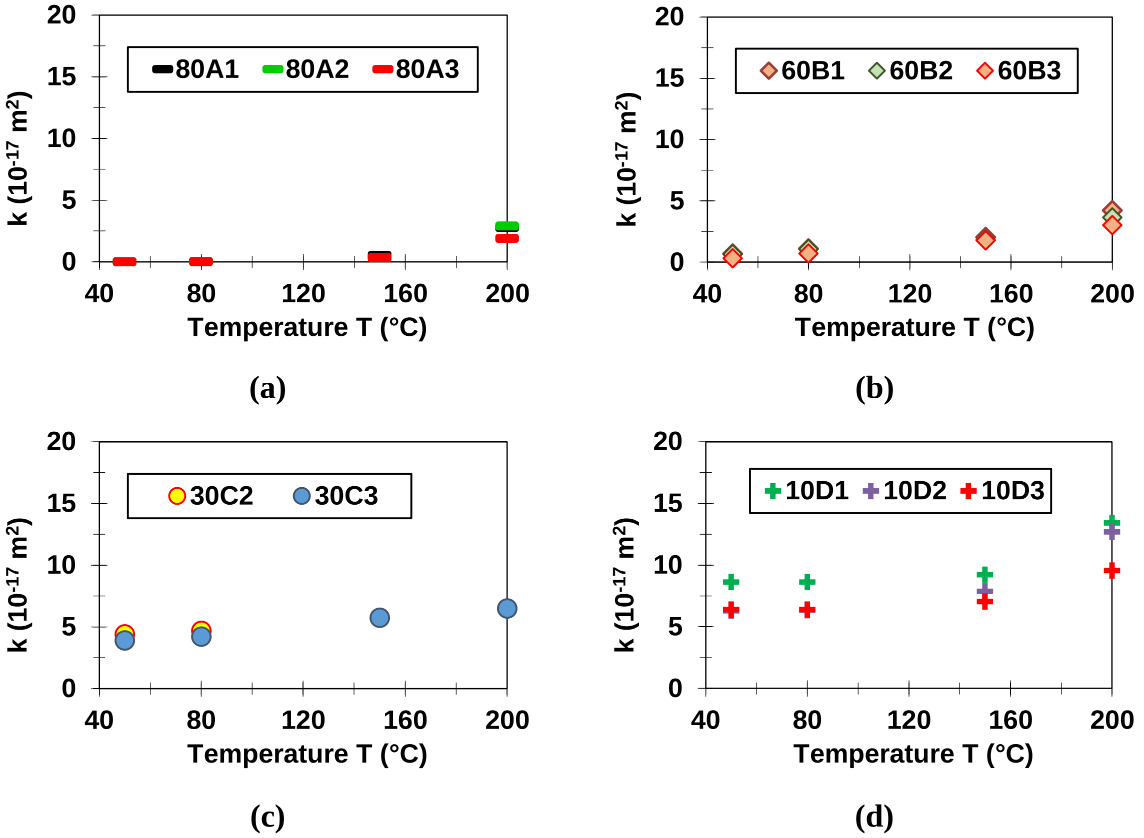

(a) (b)

(c) (d)

Figure 5. Apparent permeability as a function of the temperature for four initial saturation degrees

The flow Q(T) measured during permeability tests after thermal loading can be compared to the flow Q(50), which is the flow measured for partially saturated samples before the thermal loading. Results are presented in Figure 6. For low saturation degrees, the proportion of air flow in the initial percolation path of the concrete is higher than 60%, while, at high saturation degrees, the air flow occurs mainly in new paths induced by the thermal loading (Figure 6). This information is important for the evaluation of leakage from damaged structures in real environmental conditions.

Figure 6 is also interesting for the quantification of the cracking induced by the temperature. Crack openings were sufficient to allow significant transfer despite the high water content. Because of their size and their connection, these paths were drained even at high water contents. The air permeability is known to be a sensitive technique to detect damage [69]. For high saturation degrees, this experimentation shows that very small defects, which may have negligible impact on the mechanical properties, lead to large impact on the permeability. It confirms thus the high sensitivity of this measure to cracking, especially in saturated concrete.

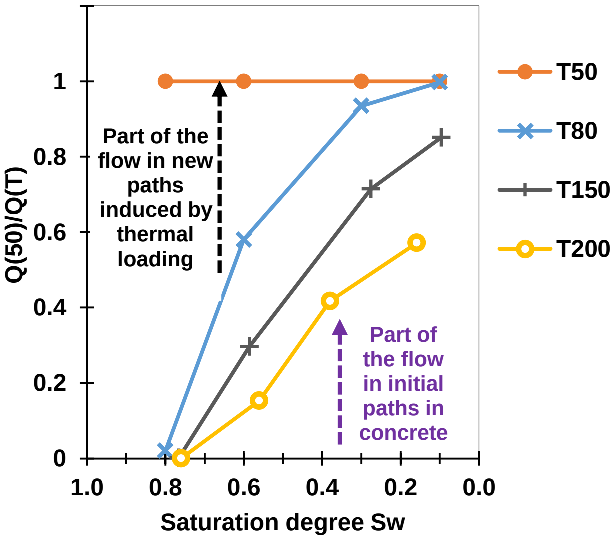

Figure 6. Ratio of the flow in samples before and after thermal loading versus the saturation degree during permeability measurement

4 Analysis

4.1 Relative change in modulus

The relative change in modulus is usually used to evaluate the concrete damage due to mechanical loading. Thermal loading leads also to relative change in modulus but the modifications are not only caused by mechanical reasons. The evolution of the modulus in concrete submitted to elevated temperatures is due to the combination of many mechanisms (cracking, physicochemical modifications, porosity saturation by pore solution). The use of relative change in modulus to evaluate the damage induced by elevated temperature in concrete is thus questionable. However, the part really due to damage in the modulus evolution is difficult to separate to the other contributions by usual measurable parameters. Therefore, the damage due to thermal loading is evaluated from relative change in modulus as is usual in modelling approaches presented in literature [10, 22]. It has not to be interpreted as the usual mechanical damage but as a global evaluation of the relative change in modulus due to all the mechanisms involved in temperature exposure. In the future, mesoscopic modelling could be used to have a better evaluation of the effects of each mechanism on the evolution of the modulus, and to distinguish clearly the mechanical damage to the contribution of other mechanisms, as particularly the water saturation of concrete porosity.

4.1.1 *Impact of drying*

The evolution of the modulus with the saturation degree was evaluated through δ_H regardless of the nature of its origins (physicochemical and/or mechanical):

$$\delta_H = 1 - \frac{E_S}{E_{100\%}} \qquad \textit{Eq. 5}$$

where δ_H is used to quantify the modulus evolution due to drying [70], E_S is the modulus at a given saturation degree (after drying), $E_{100\%}$ is the initial modulus after 60 days in lime water and before drying, taken as a reference.

For saturation degrees higher than 30%, the damage increased linearly with the saturation degree. The decrease of modulus was slightly greater than 6% for a degree of saturation of about 30% (Figure 7). This decrease is small. The impact of the water loss on the Young modulus during exposure of the concrete to the chosen temperature appears to be small until 30% of saturation is reached (drying at 60 °C).

The linearity of the damage induced by drying can be evaluated as a function of the saturation degree as follows:

$$\delta_H = H.(1 - Sw) \qquad \textit{Eq. 6}$$

The coefficient H thus defined is the rate of loss of rigidity of the material due to hydric damage. It can be used to evaluate the sensitivity of the concrete rigidity to drying: when H is high, the concrete modulus is more sensitive to loss of water.

The parameter H was calibrated using the experimental measurements. It was equal to 0.10 for the concrete tested in this work, which is in good accordance with literature results (Table 2).

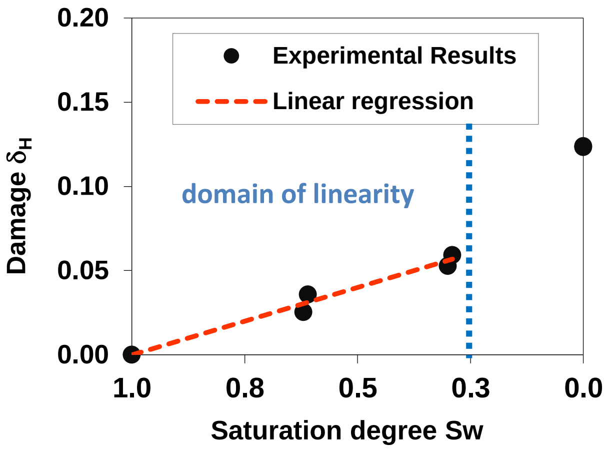

Figure 7. Damage δ_H versus saturation degree

Table 2. Value of H deduced from literature data

Concrete samples			Deduced value of H	Authors
E/C	$Rc_{100\%}$ (MPa)	$E_{100\%}$ (GPa)		
0.57	45	41	0.11	Bucher et al. [71]
0.64	32	25	0.05	Vu [72]

Most of experimental works on the evolution of Young modulus with saturation degree exhibit linearity between 100% and 20% of saturation [52, 57, 58]. For very dry materials (below 20%), the correlation between modulus and saturation can be linear [52, 58] or nonlinear [58] according to the concrete composition and test conditions. Particularly, the effect of the aggregate size on the opening of cracks due to cement paste restraint by aggregate [3] can explain a brutal increase in the impact of saturation on modulus for concrete containing coarse aggregate.

In the present work, the evolution of damage with the degree of saturation is no longer linear below 30%. In the dry state (obtained at 105 °C), the damage increases rapidly for a small difference of saturation. The loss of linearity of the Young modulus evolution indicates the creation of a cracking network having a marked impact on the permeability. For 0% of saturation (drying temperature equal to 105 °C), the concrete damage is mainly due to thermo-chemical mechanisms. Drying at high temperatures increases the importance of microcracking (density, width, length…) [43]. The density of cracking increases significantly between 50 °C and 105 °C [43]. It can explain the non-linearity of damage obtained for very small saturation degrees. However, the correlation between modulus and saturation cannot be determined for low saturation degrees as the number of measurements is not sufficient. Future works on the mechanical behaviours of concrete submitted to severe drying should focus on this domain of saturation.

Above 30% of saturation, the damage is supposed to be mainly due to water departure (impact of drying for temperatures lower than 60 °C). To quantify the damage principally associated with the water departure, it seems appropriate to keep the linear relation of the Young modulus with saturation degree. Although the nature of the cracking is different, damage of about 5% (equal to the drying damage at 30% of saturation) caused by a compressive load usually has little impact on the permeability, while damage of about 12% (equal to the drying damage at 0% of saturation) can increase the permeability by a factor lying between 2 and 5 [68, 70].

The hydric damage, as defined in this paper, does not integrate the impact of cycles of drying and re-humidification that can occur in the material on site. Additional studies are necessary to analyse the impact of the life cycle of concrete on this property.

4.1.2 Impact of elevated temperatures

The evolution of the modulus with the temperature of the thermal loading according to the initial saturation degree was evaluated through δ_{T,H_0} regardless of the nature of its origins:

$$\delta_{T,H_0} = 1 - \frac{E_{T,s}}{E_{S_0}} \qquad \textit{Eq. 7}$$

where δ_{T,H_0} is used to quantify the modulus evolution due to thermal loading in comparison with the state of samples just before the thermal loading at saturation degree Sw = S_0. E_{S_0} and $E_{T,s}$ are the modulus of concrete before and after the thermal loading, respectively.

Literature data indicate that a linear evolution can be established for the evolution of the decrease of modulus according to temperature [73]. Figure 8 illustrates the results obtained in this study. They are in good agreement with the results presented in [22].

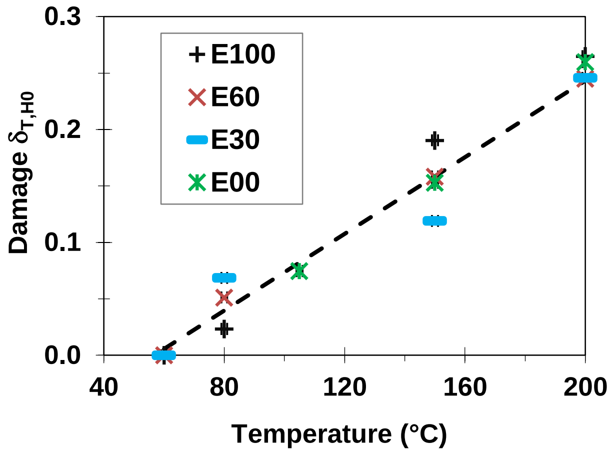

Figure 8. Evolution of the thermo-chemical damage as a function of exposure temperature

The linear regression deduced from the experiments (Figure 8) is:

$$\delta_{T,H_0} = A_{TH}.T + B_{TH} \qquad \textit{Eq. 8}$$

where A_{TH} and B_{TH} are calibration parameters. In this study, A_{TH} was equal to 0.0017 and B_{TH} to -0.0965. These values are close to parameters obtained in Schneider's work [74]. In this study, dried concrete was subjected to temperatures increasing from 20 to 800 °C [74]. From his data, A_{TH} and B_{TH} can be evaluated at 0.0011 and -0.0376 respectively.

In the last part of the paper, these results are used to analyse the correlation between the thermo-chemical damage and the evolution of the permeability induced by the exposure to temperature.

4.2 Permeability

4.2.1 Relative permeability after thermal loading

The evolution of the permeability highlighted in the previous part was caused by the combination of two mechanisms: the impact of the saturation degree on initial transfer paths and the impact of the thermo-chemical damage on the increase of the transfer path (due to decomposition of hydrates and/or cracking). In order to distinguish the two phenomena, the relative permeability $k_{TH,Rel}$ is defined in this part. In the experiments, it was almost impossible to obtain exactly the same saturation degree before and after the thermal loading and resaturation. For partially saturated concrete, a small difference of saturation degree can lead to a large variation of permeability (Figure 3). As the saturation degree was not exactly the same, experimental permeability values could not be directly compared to define $k_{TH,Rel}$. To circumvent this difficulty in the analysis, the permeability was normalized taking into account the saturation degree of concrete: $k_{TH,Rel}$ was related to the reference state obtained from the van Genuchten model and has been presented in Figure 3-b. Thus, the impact of the saturation degree was evaluated from the van Genuchten model and the impact of the thermo-chemical damage could be highlighted. For a given saturation degree S_0:

$$k_{TH,Rel} = \frac{k_{S_0T}}{k_{S_0T_0}} \qquad \textit{Eq. 9}$$

where k_{S_0T} is the permeability for a given saturation state after exposure to the chosen temperature T (80, 150 and 200 °C) and $k_{S_0T_0}$ is the reference permeability, considering the effect of the saturation degree by Eq. 4. Thus, $k_{TH,Rel}$ does not depend on the saturation degree of the sample during the permeability measurement. If the permeability is not modified by the thermal loading, $k_{TH,Rel}$ is equal to 1. If this relative permeability is higher than 1, the difference has been induced by the temperature.

Figure 9 presents the relative permeability $k_{TH,Rel}$ for samples just after the thermal loading (protocol K1).

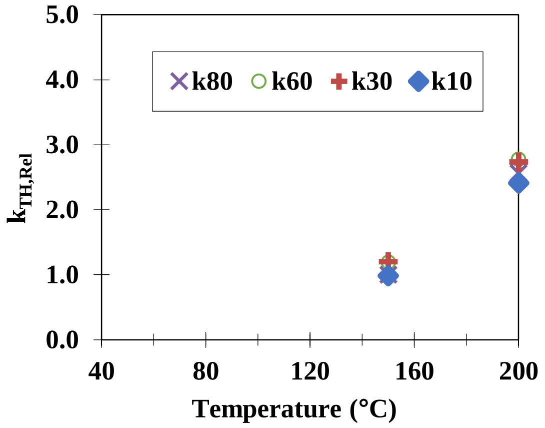

Figure 9. Relative permeability just after the thermal loading (K1)

For measurements performed just after the thermal loading (Figure 9):

- The exposure at 150 °C had a negligible impact on permeability: $k_{TH,Rel}$ is about 1.
- For the loading at 200 °C, $k_{TH,Rel}$ lies between 2 and 3. The temperature loading induced thermo-chemical damage in the concrete but the consequences in terms of permeability remain moderate at this temperature level.

For the two temperatures, the large effect on permeability shown in Figure 4 was mainly due to the decrease of the water content of the concrete.

In contrast, the impact of thermal loading on the permeability of partially saturated concrete was significant (Figure 10).

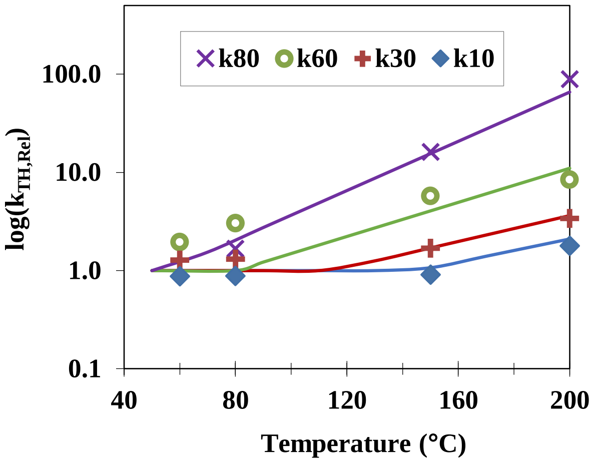

Figure 10. Relative permeability after resaturation (K2): experimentation and empirical laws

For the lowest temperature, all the relative permeability $k_{TH,Rel}$ must be equal to 1 as the samples have not been subjected to the thermal loading. However, the samples with an initial saturation degree of 60% show a mean relative permeability of about 2. This is due to an approximate evaluation of $k_{S_0T_0}$ by the van Genuchten model (differences between the model and experimental results in Figure 3-b). For the same reason, at Sw equal to 30%, $k_{TH,Rel}$ is slightly higher than 1 because the van Genuchten estimation of experimental permeability is too low. At Sw = 10%, $k_{TH,Rel}$ is less than 1 because of overestimation by the van Genuchten model.

For measurements at high saturation degrees of (60 and 80%), the impact of thermal loading at 80 °C on the permeability is quite small. If it exists, it is of the same order as the discrepancy due to the use of the van Genuchten model as explained just above. However, exposure to 200 °C leads to a significant increase in permeability. The impact of the thermal loading on permeability decreases when the initial saturation degree is lower. For high water content, significant thermo-chemical damage occurs. Even if the concrete is resaturated with the same water content, the water is not able to fill all the new paths created during the exposure to temperature. These new paths are probably micrometric and interconnected and can be drained even at high relative humidity. The consequence is a significant increase in permeability for concrete with a high saturation degree. This result is important for the evaluation of the leakage of damaged structures after exposure to elevated temperatures. Such experimental data are necessary to evaluate the capacity of mesoscopic modelling considering the impact of thermal damage on permeability [18] for partially saturated concrete.

4.2.2 Combination of saturation and thermal damage impacts

Phenomenological relationships have been proposed to evaluate the permeability of damaged concrete in relation to the initial permeability and to the temperature [7, 75]:

$$k = k_0 exp[C_T(T - T_0)] \qquad \textit{Eq. 10}$$

where k_0 is the initial permeability of concrete subjected to the reference temperature T_0 and C_T is a parameter that can be calibrated using experimental results.

The analysis proposes here to combine the van Genuchten model (Eq. 4) with the law presented in Eq. 10 to separate the impact of the saturation degree at the time of permeability measurement from the effect of the thermal damage.

With this objective, two parameters are defined:

- T_S: the temperature limit above which the thermal loading leads to an increase in permeability.

- $C_{T,S}$ is the coefficient C_T in Eq. 10 but with dependence on the initial saturation degree at the beginning of the thermal loading.

The following equation is thus proposed to evaluate the apparent permeability:

$$k_{S_0T} = \underbrace{k_0(1 - Sw)^q\left(1 - Sw^{1/m}\right)^{2m}}_{k_{S_0T_0}} . \underbrace{\exp\left[C_{T,S}\langle T-T_S\rangle\right]}_{k_{TH,Rel}} \qquad \textit{Eq. 11}$$

where $k_{S_0T_0}$ is given by the van Genuchten model, $\langle T-T_S\rangle = 0$ when $T_S > T$ and $\langle T-T_S\rangle = T - T_S$ when $T_S < T$.

$C_{T,S}$ and T_s are both calibrated to reproduce the results for each saturation degree (Figure 10) and to give a gradual trend of their evolution with the saturation degree according to:

$$C_{T,S} = A_C \exp(B_C.Sw) \qquad \textit{Eq. 12}$$

$$T_s = A_T \exp(B_T.Sw) \qquad \textit{Eq. 13}$$

where A_C, B_C, A_T, B_T are calibration parameters. For the concrete tested in this study, A_C, B_C, A_T and B_T are equal to 0.012, 0.89, 163, and -1.12 respectively.

The literature reports values of C_T lying between 0.01185 and 0.02019 [7] (for tests performed on dried samples, $S_0 = 0\%$). With Eq. 12, $C_{T,S}$ is equal to 0.012 for $S_0 = 0\%$. It is thus in good agreement with the literature values.

To obtain a good calibration (Figure 10), it seems important to replace the reference temperature T_0 in Eq. 10 by a limit temperature $T_S(Sw)$ (Eq. 13). This limit temperature depends on the initial saturation degree. Below this temperature, the thermal loading has no significant impact on the permeability. This modification was necessary to obtain a good representation of all the measurements.

For the permeability measured with the protocol K1 (measurements on dried samples just after the thermal loading), the proposed model (Eq. 11) leads to $k_{TH,Rel}$ equal to 1 and 1.8 for temperatures of 150 °C and 200 °C, respectively. Figure 9 indicates that, for T = 150 °C, $k_{TH,Rel}$ lies around 1 and, for T = 200 °C, $k_{TH,Rel}$ is about 2.5. The proposed relationship leads to a suitable evaluation of the experimental results of the first protocol.

In order to assess the rate flow of their structures, engineers in charge of the management of containment structures need phenomenological laws to evaluate the concrete permeability submitted to various loading. Such laws can also be useful for macroscopic modelling of these very large structures for which precise evaluation of cracks can be complex or too time consuming. As shown by the present analysis, the combination of two laws of the literature give a correct evaluation of this transfer property after thermal loading according to its saturation degree before exposure. The relationships proposed for the dependence of the parameters of these laws on the saturation degree allows their generalization to various environmental conditions. In this approach, concrete is supposed homogeneous without distinction of the different phases of the material and of the cracks induced by the thermal loading. More precise modelling could be helpful to better evaluate the part of the flow in the concrete porosity and in new paths formed by cracking resulting of the thermal loading. Such modelling can also be very interesting to evaluate the impact of the mechanical properties of concrete exposed to such loading on the increase of transfer property. In the future, modelling combining mechanical and transfer considerations [76] should be used to propose a more complete and precise evaluation of the effects of thermal loading on the transfer properties of concrete.

4.3 Discussion

4.3.1 Correlation between relative permeability and relative change in modulus

As the thermo-chemical damage has a linear relation with the temperature (Figure 8), the correlation between permeability and damage can be drawn from Eq. 8 and Eq. 11:

$$k_{S_0T} = \underbrace{k_0(1-Sw)^q\left(1-Sw^{1/m}\right)^{2m}}_{k_{Sr_0T_0}} . \underbrace{\exp\left[C_{T,S}\left\langle\left(\delta_{T,H_0}-B_{TH}\right)/A_{TH}-T_S\right\rangle\right]}_{k_{TH,Rel}} \qquad \textit{Eq. 14}$$

where $k_{Sr_0T_0}$ is given by the van Genuchten model.

A_{TH}, B_{TH}, $C_{T,S}$ and T_S have been calibrated in the previous parts (Eq. 8, Eq. 12 and Eq. 13).

The relative permeability $k_{TH,Rel}$ as expressed in Eq. 14 is plotted in Figure 11 for comparison with the experimental data obtained in this program.

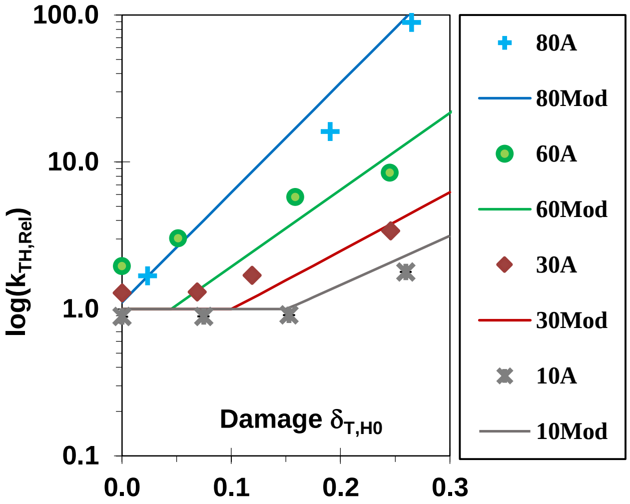

Figure 11. Comparison between experimental results and proposed model

The correlations between the relative permeability and the damage induced by the thermal loading can thus be deduced from the previous relationships (Figure 11). For low saturation degrees, the exposure to temperature leads to considerable damage but to low permeability variations. For small saturation degrees, the water in the percolation path is released and the initial permeability is already high. The relative increase after the temperature exposure is thus not so marked as for high saturation degrees.

Empirical relations (Eq. 14) can be used to evaluate the relative permeability with quite good accuracy, in relation to usual experimental dispersion for permeability and damage assessments. The distinctions between the experimental results and the predictions for the smallest damage are due to the evaluation of $k_{TH,Rel}$ as explained in the previous part (particularly for concrete at 60% of saturation).

Because of the dependence of the correlation on the saturation degree, the relative permeability cannot be directly deduced from the damage. For example, for 25% damage, the relative permeability lies between 2 and 100 according to the saturation state. For measurements on site, this correlation can be used to evaluate the relative permeability from indirect measurements. If the damage and the saturation degree of in situ concrete are known, such experimental relationships could allow the relative permeability to be evaluated without direct measurement of the permeability. Additional work will be necessary to confirm this method.

4.3.2 Comparison with literature

One of the objectives of this study was to analyse the correlation between relative permeability and damage induced by thermal loading. In the literature, such results are scarce for thermal loading lower than 200 °C and damage lower than 0.2, but several studies have analysed the impact of mechanical loading on permeability in this range of damage [31, 77]. As the damage due to mechanical and thermal loading has different origins, the consequences in terms of induced cracking and thus permeability variation have to be compared.

Figure 12 compares the results of the present study obtained on concrete subjected to thermal loading and the results of concrete subjected to mechanical compressive loading [31, 77] (obtained on concrete dried at 105 °C until constant mass). In [31, 77], the damage is calculated from $(E_0-E_d)/E_0$ with E_0, the modulus before the mechanical loading and E_d, the modulus after the mechanical loading. The relative permeability k_{Rel} is the ratio between the apparent permeabilities measured after and before the loading. For the present study, only the four trends obtained with the previous equation have been kept, to simplify the figure.

The nature and location of the damage is different according to the nature of the loading. However, thermal and mechanical loadings seem to induce similar correlations between relative permeability after loading and damage evaluated from the Young modulus (Figure 12).

The evolution of permeability according to damage is of the same order whatever the origin of the damage (mechanical or thermal). For dry concrete, mechanical loading seems to cause higher relative permeability than thermal loading.

As for compressive loading [31, 77-79], thermal loading shows a threshold of damage for unsaturated concrete. Below this threshold, the damage induced by thermal loading does not impact the permeability. The new paths induced by the thermal loading are not coalescent or not sufficiently wide to impact the permeability until this damage threshold is reached. It can be related to the threshold of crack width observed for the effect of mechanical loading on permeability [78].

For most of the experimental works, only small increases of permeability were noted for damage lower than 0.06. This is the value of damage obtained for drying to 30% of saturation (Figure 7). Drying from 60% to 30% could lead to a small increase in permeability (the maximum relative permeability is 1.8 for damage of 0.06 for all the experimental studies presented in Figure 12).

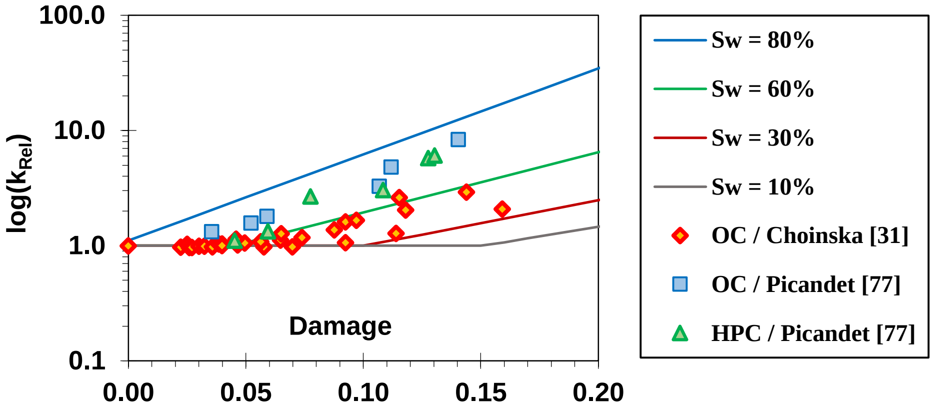

Figure 12. Evolution of permeability with damage after thermal loading (lines) and after mechanical loading (points, OC = ordinary concrete, HPC = High Performance Concrete) from [31, 77]

5 Conclusion

The findings presented in the paper can contribute to the knowledge of the evolution of concrete permeability after exposition to elevated temperatures. It deals also with the correlation between concrete damage and permeability after such loading.

Permeability of partially saturated concrete through air permeability measurement has been analysed. If the permeability is measured just after the thermal loading and drying, the initial saturation state of the concrete seems to have little impact. The permeability is then mainly impacted by the saturation state during measurement. It is thus necessary to separate the effect of thermal damage from the effect of saturation. It can be obtained after resaturation of concrete to the initial saturation degree. Permeability measurement after resaturation shows small modifications for concrete with a low saturation degree and large modifications for saturated concrete. During the thermal loading, the temperature has to be high enough to induce significant damage. This temperature limit, under which the thermal loading has no impact on concrete permeability, is dependent on the saturation degree. When the saturation degree is high, even low thermal loading may induce an increase of permeability while, when the saturation degree is low (lower than 30%), the thermal loading has to be more severe (above 100°C) before leading to a significant increase of permeability.

After exposition to elevated temperatures, air flow occurs mainly in the initial percolation path of concrete for low initial saturation degrees but the air flow occurs in new paths induced by the exposure to temperature for high initial saturation degrees. The degree of saturation of concrete on site is usually high, concrete saturated at 80% can be permeable to air after thermal loading, which was not the case before exposure. For concrete with high saturation degree, even a small damage can lead to large permeability increase.

To obtain a good representation of all the saturation degrees (from 10% to 100%), it has been necessary to revisit the usual empirical relations between permeability and temperature. A van Genuchten model cannot be used alone to predict the permeability of saturated concrete damaged by thermal loading. It can be combined with a phenomenological model to account of the increase of permeability due to thermo-chemical damage. Adaptations of existing laws have been proposed in this paper to take the impact of the initial saturation degree into account.

These experimental data and analysis are necessary to obtain relevant modelling to predict the behaviour of structures in field after thermal loading due, for example, to accidental situation.

6 Acknowledgements

The authors acknowledge the financial support provided by the project “Non-destructive evaluation of containment of nuclear power plants” (ENDE) financed by the Programme Investissement d’Avenir (PIA – Centre National de la Recherche Scientifique, délégation Provence et Corse, France). The opinions presented in this paper reflect only those of the authors and do not necessarily represent the opinions of the funding agencies.

7 References

[1] Z. P. Bazant and P. C. Prat, “Effect of Temperature and Humidity on Fracture Energy of Concrete,” Mater. J., vol. 85, no. 4, pp. 262–271, 1988.

[2] N. Burlion, I. Yurtdas, and F. Skoczylas, “Comportement mécanique et séchage de matériaux à matrice cimentaire ; Comparaison mortier - béton,” Rev. Fr. Génie Civ., vol. 7, no. 2, pp. 145–165, 2003.

[3] M. Szczesniak, T. Rougelot, N. Burlion, J. Shao, “Compressive strength of cement-based composites : Roles of aggregate diameter and water saturation degree,” Cem. Concr. Compos., Vol. 37, pp. 249–258, 2013.

[4] I. Yurtdas, N. Burlion, and F. Skoczylas, “Experimental characterisation of the drying effect on uniaxial mechanical behaviour of mortar,” Mater. Struct., vol. 37, no. 3, pp. 170–176, 2004.

[5] S. Divya Rani, M. Santhanam, “Influence of moderately elevated temperatures on engineering properties of concrete used for nuclear reactor vaults”, Cem. Concr. Compos., vol. 34, pp. 917–923, 2012.

[6] Y. Pei, F. Agostini, and F. Skoczylas, “The effects of high temperature heating on the gas permeability and porosity of a cementitious material,” Cem. Concr. Res., vol. 95, pp. 141–151, 2017.

[7] D. Gawin, C. Alonso, C. Andrade, C. E. Majorana, and F. Pesavento, “Effect of damage on permeability and hygro-thermal behaviour of HPCs at elevated temperatures: Part 1. Experimental results,” Comput. Concr., vol. 2, no. 3, pp. 189–202, 2005.

[8] N. Hearn, “Effect of Shrinkage and Load-Induced Cracking on Water Permeability of Concrete,” Mater. J., vol. 96, no. 2, pp. 234–241, 1999.

[9] N. Burlion, F. Skoczylas, and T. Dubois, “Induced anisotropic permeability due to drying of concrete,” Cem. Concr. Res., vol. 33, no. 5, pp. 679–687, 2003.

[10] S. D. Pont, B. A. Schrefler, and A. Ehrlacher, “Intrinsic Permeability Evolution in High Temperature Concrete : An Experimental and Numerical Analysis,” Transp. Porous Media, vol. 60, no. 1, pp. 43–74, 2004.

[11] M. Lion, F. Skoczylas, Z. Lafhaj, and M. Sersar, “Experimental study on a mortar. Temperature effects on porosity and permeability. Residual properties or direct measurements under temperature,” Cem. Concr. Res., vol. 35, no. 10, pp. 1937–1942, 2005.

[12] T. Suzuki, K. Takiguchi, and H. Hotta, “Leakage of gas through concrete cracks,” Nucl. Eng. Des., vol. 133, no. 1, pp. 121–130, 1992.

[13] G. A. Khoury, B. N. Grainger, and P. J. Sullivan, “Transient thermal strain of concrete: literature review, conditions within specimen and behaviour of individual constituents,” Mag. Concr. Res., vol. 37, no. 132, pp. 131–144, 1985.

[14] I. Hager, “Behaviour of cement concrete at high temperature,” Bull. Pol. Acad. Sci. Tech. Sci., vol. 61, no. 1, pp. 145–154, 2013.

[15] A. Noumowé, “Effet de hautes températures (20-600°C) sur le béton : cas particulier du béton à hautes performances,” Ph.D. Thesis, INSA de Lyon, 1995.

[16] T. Z. Harmathy, “Thermal properties of concrete at elevated temperatures’, J. Mater., 1970.

[17] P. Klieger, J. F. Lamond, “Significance of test and properties of concrete and concrete-making materials”, ASTM Publication, USA, 1994.

[18] F. Grondin, H. Dumontet, A. Ben Hamida, H. Boussa, “Micromechanical contributions of the behaviour of cement-based materials: Two-scale modelling of cement paste and concrete in tension at high temperatures”, Cem. Concr. Compos., vol. 33, pp. 424–435, 2011.

[19] M. V. G. de Morais, A. Noumowé, M. Kanema, J.-L. Gallias, and R. Cabrillac, “Transferts thermo-hydriques dans un élément en béton exposé à une température élevée: Approches numérique et expérimentale,” 24ème Rencontres Univ. Génie Civ. AUGC06, pp. 1–10, 2006.

[20] J.-C. Mindeguia, P. Pimienta, A. Noumowé, and M. Kanema, “Temperature, pore pressure and mass variation of concrete subjected to high temperature — Experimental and numerical discussion on spalling risk,” Cem. Concr. Res., vol. 40, no. 3, pp. 477–487, 2010.

[21] Z. P. Bažant, “Constitutive equation for concrete creep and shrinkage based on thermodynamics of multiphase systems,” Matér. Constr., vol. 3, no. 1, pp. 3–36, 1970.

[22] D. Gawin, F. Pesavento, and B. A. Schrefler, “Modelling of hygro-thermal behaviour of concrete at high temperature with thermo-chemical and mechanical material degradation,” Comput. Methods Appl. Mech. Eng., vol. 192, no. 13–14, pp. 1731–1771, 2003.

[23] Z. P. Bazant and F. H. Wittmann, “Creep and shrinkage in concrete structures,” 1982.

[24] D. Gardner, “Experimental and numerical studies of the permeability of concrete,” Ph.D. Thesis, Cardiff University, 2005.

[25] M. A. Sanjuán and R. Muñoz-Martialay, “Oven-drying as a preconditioning method for air permeability test on concrete,” Mater. Lett., vol. 27, no. 4–5, pp. 263–268, 1996.

[26] D. Stark, “The moisture condition of field concrete exhibiting alkali-silica reactivity,” in *Durability of concrete. G. M. IDORN International Symposium*, 1992, pp. 973–987.

[27] J. Verdier, “Contribution à la caractérisation de l’évolution du taux de fuite des enceintes de confinement du parc nucléaire,” PhD Thesis, Université Paul Sabatier, Toulouse, France, 2001.

[28] L. Granger, “Comportement différé du béton dans les enceintes de centrales nucléaires: analyse et modélisation,” PhD Thesis, Ecole Nationale des Ponts et Chaussées, Marne-La-Vallée, France, 1996.

[29] S. Goto, D.M. Roy, “The effect of W/C ratio and curing temperature on the permeability of hardened cement paste,” Cem. Concr. Res., vol. 11, pp. 575–579, 1981.

[30] M. Jooss, H.W. Reinhardt, “Permeability and diffusivity of concrete as function of temperature,” Cem. Concr. Res., vol. 32, pp. 1497–1504, 2002.

[31] M. Choinska, A. Khelidj, G. Chatzigeorgiou, and G. Pijaudier-Cabot, “Effects and interactions of temperature and stress-level related damage on permeability of concrete,” Cem. Concr. Res., vol. 37, no. 1, pp. 79–88, 2007.

[32] A.N. Noumowe, R. Siddique, G. Debicki, “Permeability of high-performance concrete subjected to elevated temperature (600 °C),” Constr. Build. Mater., vol. 23, pp. 1855–1861, 2009.

[33] F. Jacobs, “Permeability to gas of partially saturated concrete,” Mag. Conc. Res., vol. 50, pp. 115-121, 1998.

[34] A. Abbas, M. Carcasses, and J.-P. Ollivier, “Gas permeability of concrete in relation to its degree of saturation,” Mater. Struct., vol. 32, no. 1, pp. 3–8, 1999.

[35] Z. A. Kameche, F. Ghomari, M. Choinska, and A. Khelidj, “Assessment of liquid water and gas permeabilities of partially saturated ordinary concrete,” Constr. Build. Mater., vol. 65, pp. 551–565, 2014.

[36] H. Kallel, “Effet du degré de saturation et de la température sur le comportement mécanique du béton,” in 13ème Journées d’études des Milieux Poreux, 2016.

[37] E. Oukhemanou, S. Desforges, E. Buchoud, S. Michel-Ponnelle, A. Courtois, “VeRCoRs Mock-Up: Comprehensive Monitoring System for Reduced Scale Containment Model,” Technological Innovations in Nuclear Civil Engineering TINCE, 2016, Paris, France.

[38] H. E. A. Sogbossi, “Etude de l’évolution de la perméabilité du béton en fonction de son endommagement : transposition des résultats de laboratoire à la prédiction des débits de fuite sur site,” Ph.D. Thesis, Université de Toulouse, Université Toulouse III - Paul Sabatier, 2017.

[39] V. Waller, “Relations entre composition des betons, exothermie en cours de prise et resistance en compression,” ENPC, 1999.

[40] C. Antón, M. A. Climent, G. de Vera, I. Sánchez, and C. Andrade, “An improved procedure for obtaining and maintaining well characterized partial water saturation states on concrete samples to be used for mass transport tests,” Mater. Struct., vol. 46, no. 8, pp. 1389–1400, 2012.

[41] RILEM TC 116-PCD, “Permeability of concrete as a criterion of its durability, final report,” Mater. Struct., vol. 32, no. 217, pp. 163–173, 1999.

[42] M. Carcassès, A. Abbas, J.-P. Ollivier, and J. Verdier, “An optimised preconditioning procedure for gas permeability measurement,” Mater. Struct., vol. 35, no. 1, pp. 22–27, 2002.

[43] Z. Wu, H.S. Wong, N.R. Buenfeld, “Influence of drying-induced microcracking and related size effects on mass transport properties of concrete,” Cem. Concr. Res., vol. 68, pp. 35–48, 2015.

[44] NF EN 12390-3, “Essais pour béton durci - Partie 3 : résistance à la compression des éprouvettes,” AFNOR, 2003.

[45] RILEM TC, RILEM Recommendations for the Testing and Use of Constructions Materials - CPC 8 Modulus of elasticity of concrete in compression, 1994.

[46] J. J. Kollek, “The determination of the permeability of concrete to oxygen by the Cembureau method-a recommendation,” Mater. Struct., vol. 22, no. 3, pp. 225–230, 1989.

[47] Norme XP P18-463, Norme XP P18-463 - Essai pour béton durci - Essai de perméabilité à l’air. 1999.

[48] V. Garnier, C. Payan, L. Martin et al., “Non-destructive evaluation of containment walls in nuclear power plants,” 43rd annual review of progress in quantitative nondestructrive evaluation, Vol. 36, AIP Conference Proceedings, 1806(1):080018, 2017.

[49] B. Masson, “Démarche industrielle de compréhension des phénomènes de transferts dans les parois en béton,” 31èmes Rencontres de l’AUGC, ENS Cachan, 2013.

[50] S. Medjigbodo, A. Darquennes, C. Aubernon, A. Loukili, “Effects of the air – steam mixture on the permeability of damaged concrete,” Cem. Concr. Res., vol. 54, pp. 98–105, 2013.

[51] S. Pihlajavaara, “A review of some of the main results of a research on the ageing phenomena of concrete: effect of moisture conditions on strength, shrinkage and creep of mature concrete,” Cem. Concr. Res., vol. 4, pp. 761–771, 1974.

[52] V. Kanna, O. RA, J. HM, “Effect of shrinkage and moisture content on the physical characteristics of blended cement mortarts,” Cem. Concr. Res., vol. 28, pp. 1467–1477, 1998.

[53] I. Yaman, N. Hearn, H. Aktan, “Active and non-active porosity in concrete Part I : Experimental evidence,” Mater. Struct., vol. 35, pp. 102–109, 2002.

[54] I. Yurtdas, N. Burlion, and F. Skoczylas, “Triaxial mechanical behaviour of mortar: Effects of drying,” Cem. Concr. Res., vol. 34, no. 7, pp. 1131–1143, 2004.

[55] N. Burlion, F. Bourgeois, J. Shao, “Effects of desiccation on mechanical behaviour of concrete,” Cem. Concr. Compos., vol. 27, pp. 367–379, 2005.

[56] G. Villain, L. Le Marrec, and L. Rakotomanana, “Determination of the bulk elastic moduli of various concretes by resonance frequency analysis of slabs submitted to impact echo,” Eur. J. Environ. Civ. Eng., vol. 15, no. 4, pp. 601–617, 2011.

[57] I. Maruyama, H. Sasano, Y. Nishioka, G. Igarashi, “Strength and Young’s modulus change in concrete due to long-term drying and heating up to 90 °C,” Cem. Concr. Res., vol. 66, pp. 48–63, 2014.

[58] W. Wang, C. Lu, G. Yuan, Y. Zhang, “Effects of pore water saturation on the mechanical properties of fly ash concrete,” Constr. Build. Mater., vol. 130, pp. 54–63, 2017.

[59] I. Yurtdas, N. Burlion, J.-F. Shao, and A. Li, “Evolution of the mechanical behaviour of a high performance self-compacting concrete under drying,” Cem. Concr. Compos., vol. 33, no. 3, pp. 380–388, 2011.

[60] H. Sogbossi, J. Verdier, and S. Multon, “Impact of reinforcement-concrete interfaces and cracking on gas transfer in concrete,” Constr. Build. Mater., vol. 157, pp. 521–533, 2017.

[61] G. Torelli, P. Mandal, M. Gillie, and V.-X. Tran, “Concrete strains under transient thermal conditions: A state-of-the-art review,” Eng. Struct., vol. 127, pp. 172–188, 2016.

[62] K. Li, M. Stroeven, P. Stroeven, L. J. Sluys, “Effects of technological parameters on permeability estimation of partially saturated cement paste by a DEM approach, Cem. Concr. Compos., vol. 84, pp. 222–231, 2017.

[63] J. Verdier and M. Carcassès, “Equivalent gas permeability of concrete samples subjected to drying,” Mag. Concr. Res., vol. 56, no. 4, pp. 223–230, 2004.

[64] M. T. V. Genuchten, “A Closed-form Equation for Predicting the Hydraulic Conductivity of Unsaturated Soils 1,” Soil Sci. Soc. Am. J., vol. 44, no. 5, pp. 892–898, 10/01 1980.

[65] L. Jason, “Relation endommagement perméabilité pour les bétons : application aux calculs de structures,” PhD Thesis, Université de Nantes, 2004.

[66] V. Baroghel-Bouny, “Caractérisation microstructurale et hydrique des pâtes de ciment et des bétons ordinaires et à très hautes performances,” Ph.D. Thesis, Ecole Nationale des Ponts et Chaussées, 1994.

[67] J. P. Monlouis-Bonnaire, J. Verdier, and B. Perrin, “Prediction of the relative permeability to gas flow of cement-based materials,” Cem. Concr. Res., vol. 34, no. 5, pp. 737–744, 2004.

[68] M. Choinska, “Effets de la température, du chargement mécanique et de leurs interactions sur la perméabilité du béton de structure,” PhD Thesis, Ecole Centrale de Nantes; Université de Nantes, 2006.

[69] F. Ghasemzadeh, R. Rashetnia, D. Smyl, M. Pour-Ghaz, “A comparison of methods to evaluate mass transport in damaged mortar”, Cem. Concr. Compos., vol. 70, pp. 119–129, 2016.

[70] V. Picandet, “Influence d’un endommagement mécanique sur la perméabilité et sur la diffusivité hydrique des bétons,” PhD Thesis, Ecole Centrale de Nantes, 2001.

[71] R. Bucher, T. Vidal, A. Sellier, and J. Verdier, “Effet du séchage sur les propriétés mécaniques des matériaux cimentaires,” in 23ème Congrès Français de Mécanique, 2017.

[72] X. H. Vu, ‘Caractérisation expérimentale du béton sous fort confinement : influences du degré de saturation et du rapport eau/ciment’, PhD Thesis, Université Joseph-Fourier-Grenoble I, 2007.

[73] P. Chhun, “Modélisation du comportement thermo-hydro-chemo-mécanique des enceintes de confinement nucléaire en béton armé-précontraint,” PhD Thesis, Université Toulouse III-Paul Sabatier, 2017.

[74] U. Schneider, “Concrete at high temperatures — A general review,” Fire Saf. J., vol. 13, no. 1, pp. 55–68, 1988.

[75] Z. P. Bažant and W. Thonguthai, “Pore Pressure and Drying of Concrete at High Temperature,” J. Eng. Mech. Div., vol. 104, no. 5, pp. 1059–1079, 1978.

[76] S. Rahal, A. Sellier, G. Casaux-Ginestet, “Finite Element Modelling of permeability in brittle materials cracked in tension,” Int. J. Solids Struct., vol. 113–114, pp. 85–99, 2017.

[77] V. Picandet, A. Khelidj, and G. Bastian, “Effect of axial compressive damage on gas permeability of ordinary and high-performance concrete,” Cem. Concr. Res., vol. 31, no. 11, pp. 1525–1532, 2001.

[78] M. Hoseini, V. Bindiganavile, N. Banthia, “The effect of mechanical stress on permeability of concrete: A review”, Cem. Concr. Compos., vol. 31, pp. 213–220, 2009

[79] S. Rahal, A. Sellier, and J. Verdier, “Modelling of change in permeability induced by dilatancy for brittle geomaterials,” Constr. Build. Mater., vol. 125, pp. 613–624, 2016.